

TECHNICAL ARTICLE

Composition and Operation of a Semi-Virtual Renewable Energy-based Building Emulator

Simo Kilpeläinen*, Minyan Lu†, Sunliang Cao‡, Ala Hasan§ and Shuqin Chen†

This paper describes the composition and operation of a semi-virtual energy system and building emulator designed for studying hybrid grid interactions of a modern nearly-zero energy building.

The system consists of a real part for energy production (PV panels and micro-wind turbine), storage (batteries and hot water storage tanks) and conversion (ground-source heat pump GSHP and electric heater) combined with a virtual part that models a single-family house in the computer simulation program TRNSYS. A Labview program is used for communication between the real and virtual parts.

Measurement data from six periods selected for study between September 2015 and February 2016 are analyzed. The data indicate that during the study, the total electricity consumption was 1290 kWh, divided to 44/38/18% between household appliances, GSHP and electric heater, respectively. The local net production was 250 kWh, or 19% of the total demand. PV, which was heavily concentrated in fall, accounted for 54% of the production. Wind production was winter-centered.

The electrical energy matching aspects of the system are represented with two indices: OEFe (on-site electrical energy fraction), the fraction of the building electrical demand covered by local production, and OEMe (on-site electrical energy matching), the ratio of the building's self-consumption to the total local production. The matching capability of the energy system was found poor due to daily and seasonal mismatches between production and demand. The small net production compared to demand led to small OEFe and large OEMe values overall.

Keywords: nearly zero-energy buildings; energy matching; renewables; building emulation

Introduction

Buildings account for roughly 40% of the total energy use within the European Union (European Commission, 2017a). To lessen the dependency on fossil fuels and to reduce greenhouse gas emissions, the European Commission set a directive on the energy performance of buildings in 2010 which requires all new buildings within the union to be nearly-zero energy buildings by the end of 2020 (European Commission, 2017b). To comply with this directive, local renewable energy production systems such as PV panels, micro-wind turbines, solar thermal collectors or other similar devices need to be integrated into the network either at building or community level.

The energy production from renewable sources (sun and wind) is sporadic and unpredictable so there is a challenge to maintain the balance between supply and demand in

both electrical and heating/cooling grids, especially in the future when a larger fraction of the energy production is to be covered by renewables. In such a scenario, smart energy systems that are able to communicate with the supply grids and adjust/direct both local production and demand in real-time become essential to achieve the desired outcome (Delucchi & Jacobson 2011; Pina, Silva & Ferrao 2012; Sorensen 2007; Ueckerdt, Brecha & Luderer 2015).

Several studies on how to address the matching issue in grids that are largely reliant on renewable energy sources have been made from the supply point-of-view (Bussar 2015; Krajačić et al. 2011; Luthra 2014; Plessmann 2014), demand point-of-view (Cao, Hasan & Sirén 2013a; Korkas et al. 2016; Xue et al. 2014) and considering both sides (Cao, Hasan & Sirén 2013b; Wang et al. 2014). Also, since small-scale renewable energy generation systems are becoming more common with the concept of zero-energy buildings, the role of prosumers with two-way grid connections has been an increasingly studied research topic (Hirvonen et al. 2016; Lund, Marszal-Pomianowska & Heiselberg 2011; Salom et al. 2014). These studies have brought a large amount of knowledge related to various aspects of the supply-demand interactions in renewable

* Aalto University School of Engineering, FI-00076 Aalto, FI

† College of Architecture and Civil Engineering, Zhejiang University, Hangzhou, CN

‡ Department of Building Services Engineering, The Hong Kong Polytechnic University, HK

§ VTT Technical Research Centre of Finland, FI-02044 VTT, FI

Corresponding author: Simo Kilpeläinen (simo.kilpelainen@aalto.fi)

energy grids. However, experimental studies are very few and all of them are conducted based on data monitored at an hourly interval. The time resolution can have a large effect when the matching capability of a PV- or wind-based energy system is considered (Cao & Sirén 2014; Cao & Sirén 2015) so there is a gap to fulfill.

In this paper, a semi-virtual emulator platform consisting of several local renewable energy systems (PV panels, micro-wind turbine and ground source heat pump) and a simulated nearly zero-energy residential building is established to study the energy supply-demand interactions with real-time monitored data at a high time resolution over a full calendar year in Finnish climate conditions.

The novelty of the research comes from the operation principle and use of the emulator platform. While there are similar semi-virtual test platforms in other laboratories (IEA Annex 67, 2017), the one presented in this paper operates in a distinctly different manner. The other platforms presented in the IEA Annex 67 report are mainly used for benchmarking energy solutions e.g. heat pumps, PV panels etc. and are typically run for a few days or weeks at a time whereas the platform presented in this paper operates year round and is subject to real-time weather changes.

The aim of this paper is to give a description of the emulator platform and its components and analyze its operation. Experimental results from the first year operation of the emulator platform are presented and discussed with respect to energy demand, local renewable production

and finally the matching of the demand and production. The analysis is conducted based on data recorded between Sep 2015 and Feb 2016. Since there were some gaps in the data, seven consecutive days from each month were chosen as the studied periods.

Description of the System

The semi-virtual emulator platform at Aalto University, located in Espoo- Finland, consists of both real components and virtual ones running in a computer simulation. An overview of the system is presented in **Figure 1**. Energy production, conversion and storage are realized with physical equipment whereas the building heating and electricity loads are simulated.

For electricity production, there are 18 unbranded German-made poly-Si photovoltaic panels supplied by Finnwind company, each 240 W_p (total peak power 4.32 kW) installed at a 45-degree inclination facing south, and a four-kilowatt Finnwind Tuule E200 micro-wind turbine on top of a nine-meter mast on the roof of the laboratory hall (Finnwind Oy, 2017). The power curve of the micro-wind turbine is shown in **Figure 2**. The PV panels and the micro-wind turbine are connected into a local island grid with SMA Sunny Island 6.0H inverters (SMA Solar Technology AG, 2017). Surplus electricity can either be stored in four RITAR AGM RA12-200D 12 V, 200 Ah valve-regulated lead acid (VRLA) batteries connected in series (system voltage 48 V), or fed to the electricity grid (RITAR Power, 2017). The grid connection is

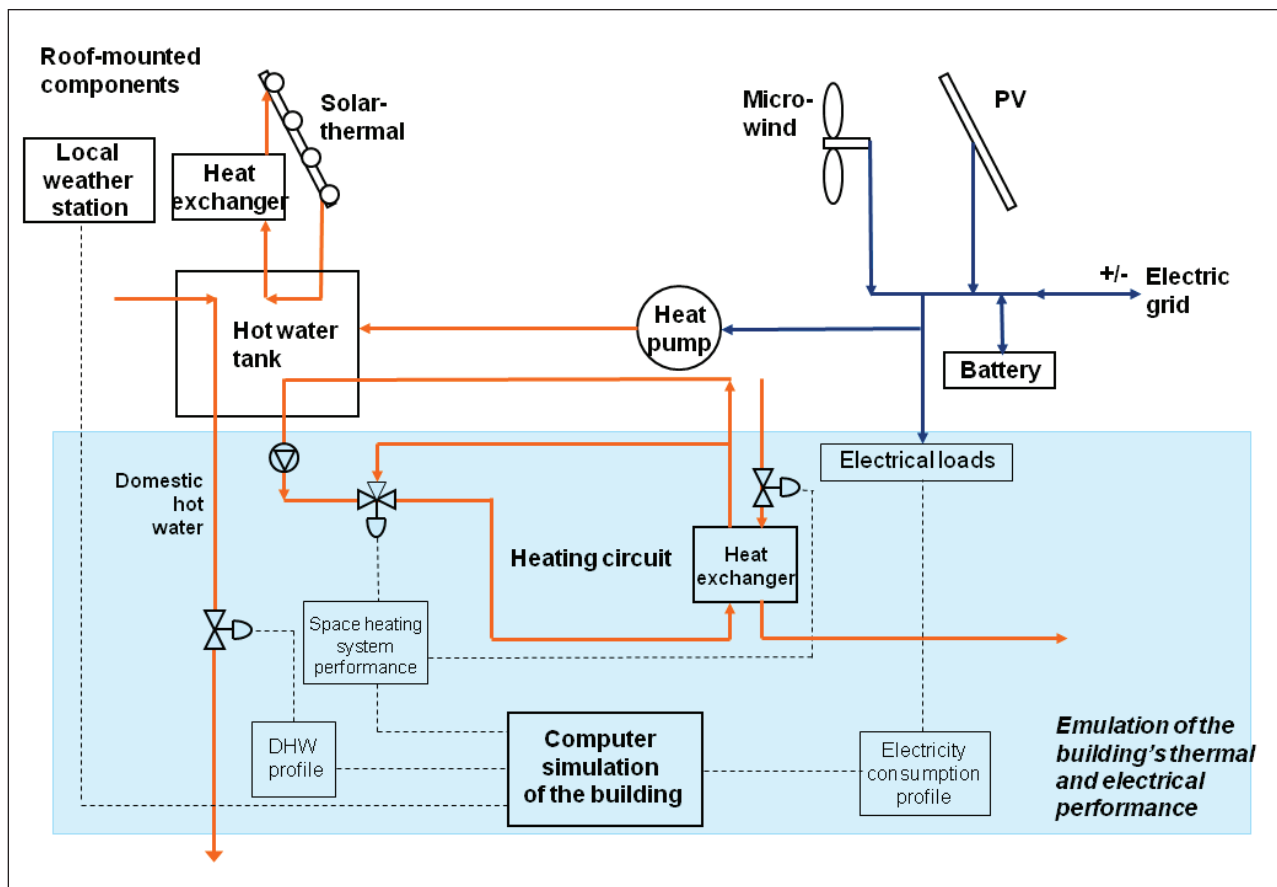


Figure 1: Overview of the emulator system.

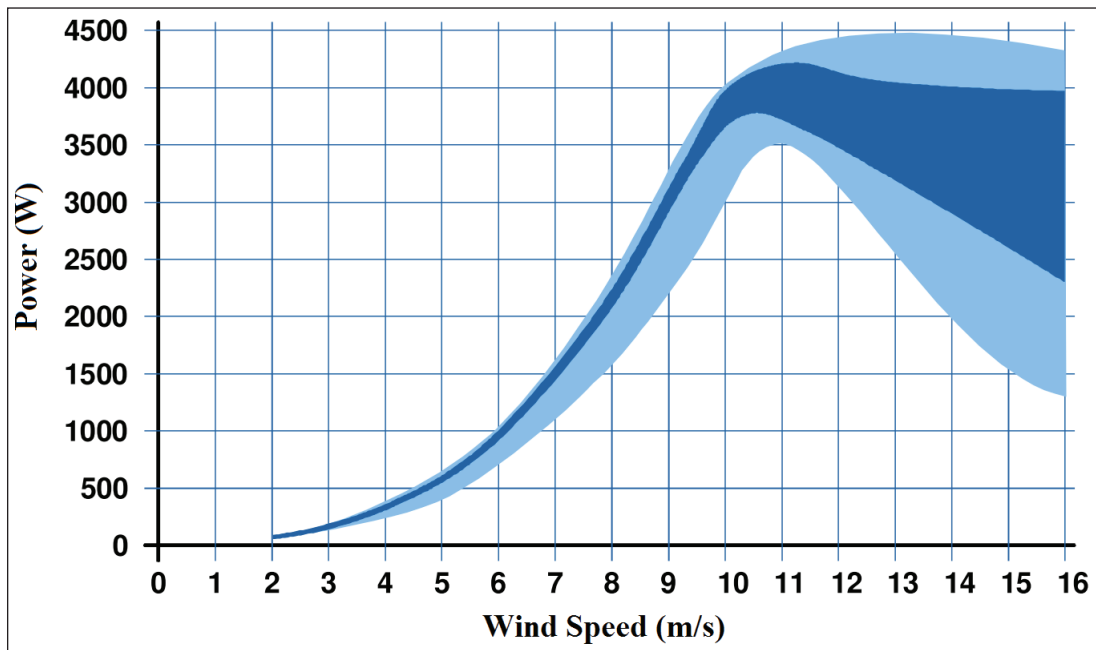


Figure 2: Power curve of the Finnwind Tuule E200 micro-wind turbine (Finnwind Oy, 2011).

currently virtual and the exported electricity is dissipated via artificial loads.

Heat is produced with a five-kilowatt Oilon Geopro 5 GT ground source heat pump (GSHP) which is no longer available for sale and has been replaced by the Junior GT model (Oilon Group Oy, 2017). For heat storage, there are three Akvaterm AKVA SOLAR hot water storage tanks (Akvaterm Oy, 2014). Two of the tanks have a capacity of 500 litres and the third one 300 litres. One of the 500 litre tanks is equipped with an electric heater (6 kW) to ensure that the domestic hot water temperature meets the legionella regulations of the Finnish Building Code D1 (Finnish Ministry of the Environment 2007) at all times. In this study, only the 500 litre tank with the electric heater was utilized.

All the real components in the system are sized according to what would be a typical setup in a Finnish single-family house, and no optimization has been done regarding matching the production with the loads of the building as the purpose of the platform is to investigate system interactions in a realistic setting. Also, the installation location of the renewable production systems (PV panels and microwind turbine) is far from optimal due to shading and obstruction from trees, rooftop installations etc.

The virtual part of the system is realized with TRNSYS software (The University of Wisconsin 2017). The simulated parts are the building under investigation and the GSHP borehole. The simulated building in this paper was a standard well-insulated two-storey Finnish single-family house with a total floor area of 150 m² (Cao, Hasan & Sirén 2013a). The simulations were run in real-time based on typical weather and energy consumption profiles of electrical appliances that fulfil the Finnish Building Code annual values.

The real and virtual parts are connected by an NI Labview-based program, which also acts as a user interface for

the emulator platform. The program both monitors the real components with the help of over 100 temperature, voltage, current and flow sensors, and generates high-precision voltage signals to control the actuators of the system. The communication between the TRNSYS and Labview programs is handled via text files.

Energy Demand of the Building

Electricity Demand

The electricity demand of the building can be divided into three main parts: appliances, heat pump and the hot water tank electric heater. Appliances in this context mean household equipment (such as washing machine, stove and dishwasher) as well as lighting and ventilation fans. In this project, this part was simulated with a detailed TRNSYS model based on typical household equipment usage profiles with annual values in accordance with the Finnish Building Code, and a reference weather file compiled from several years of historic Helsinki weather data (Kalamees, et al., 2012). The heat pump and the electric heater are present as real components in the system so their consumption was measured during the operation.

The total electricity consumption for the six periods under investigation in Sep 2015–Feb 2016 was 1290 kWh (or 8.6 kWh/m²). The largest share of this total belonged to the appliances at 44% but the heat pump was the largest single consumer at 38%. The remaining 18% was consumed by the electric heater. When looking at the consumption split into the six periods under investigation (**Figure 3**), the demand from the appliances stayed almost constant during each month whereas the electric heater and especially the heat pump were more used during the cold winter months when more heating was needed.

The consumption profiles at hourly intervals for each studied period (**Figure 4**) reveal a trend for the appliances that is repeated throughout the monitored period. The

baseline demand due to equipment running all the time (fridge, freezer, devices on standby and HVAC equipment) was around 200 W and each day there were two peak periods from 6:00 to 9:00 and from 17:00 to 24:00, corresponding to times when the occupants were at home. The electricity use during the morning peak ranged from 500 to 780 W whereas the peak in the evening was larger at 800 to 1500 W. In the weekend one of the evening peaks was much higher, around 5500 W, due to the operation of the sauna stove.

The seasonal variation in the use of the GSHP is clearly visible in **Figure 4**. In the studied period in September, there were seven operation cycles and thus the heat pump was operated only once per day for 80 minutes on average. When moving towards winter, the number of operation cycles and their lengths gradually increased. In October, there were 13 ~ 100-minute cycles, almost two per day, whereas in November–February the numbers of cycles were 19, 24, 25 and 21, respectively, amounting to three or more per day with the cycle length varying from 120 to over 200 minutes.

The electric heater, whose only function is to ensure that the temperature of the domestic hot water (DHW) is kept in compliance with the Finnish legionella regulations at a minimum of 60°C, was operated from two to five minutes per hour, always in conjunction with the DHW use.

Heating Demand

The heating demands of both space heating and domestic hot water use were obtained from the TRNSYS simulations and fed to the real system. The domestic hot water usage profile was modified so that the water ran only for three minutes at the beginning of every hour. This was done to ensure overall correct flow rates as the real, sporadic DHW

use could not have been replicated with the valves and flow sensors present in the system. To obtain the real consumption of the building, the amounts of heating energy were calculated based on the out-/inlet temperatures and flow rates of the space heating and domestic hot water loops in the emulator.

The total heat consumption for the whole studied period was 1280 kWh, with space heating accounting for three quarters and DHW use for the rest. The DHW use, as expected, had little variation throughout the studied periods, with the consumption ranging from 45 kWh in September to 65 kWh in January. On the other hand, the space heating demand varied a lot from less than 30 kWh during the period in September to more than 300 kWh during the period in January, as can be seen from **Figure 5**.

The hourly data shown in **Figure 6** reveals that the DHW use follows a similar trend each day during September–December. At night, there was no consumption at all, and in the morning at around seven the consumption started from 150 W and increased steadily to 450 W at 11. During midday, approximately from 11 to 14, the DHW usage dropped to 350 W. After that it increased back to 450 W and stayed there until late in the evening. For January and February, the trend was otherwise similar but in the evening, between 20 and 21, there was an additional sharp increase that peaked at 1150 W.

The hourly data reveals the strong dependency of the space heating demand on the outside air temperature even within the same period. Especially during the cold winter months, there were large differences between the required heating powers. In September, there was very low demand for space heating but between October and February it was constantly in operation with the

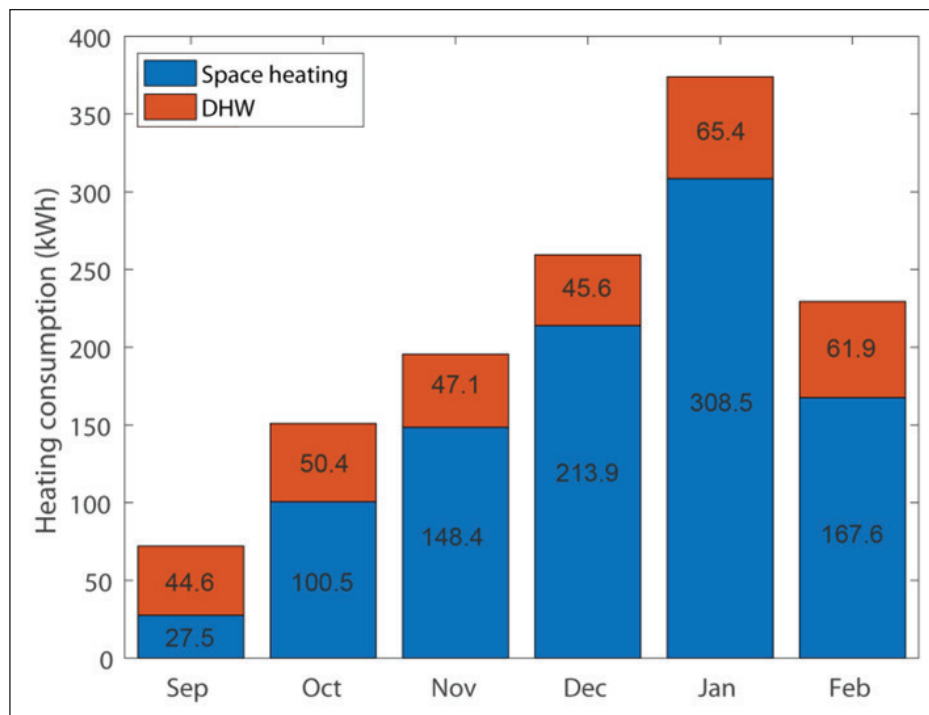


Figure 5: Heat consumption for the six studied periods.

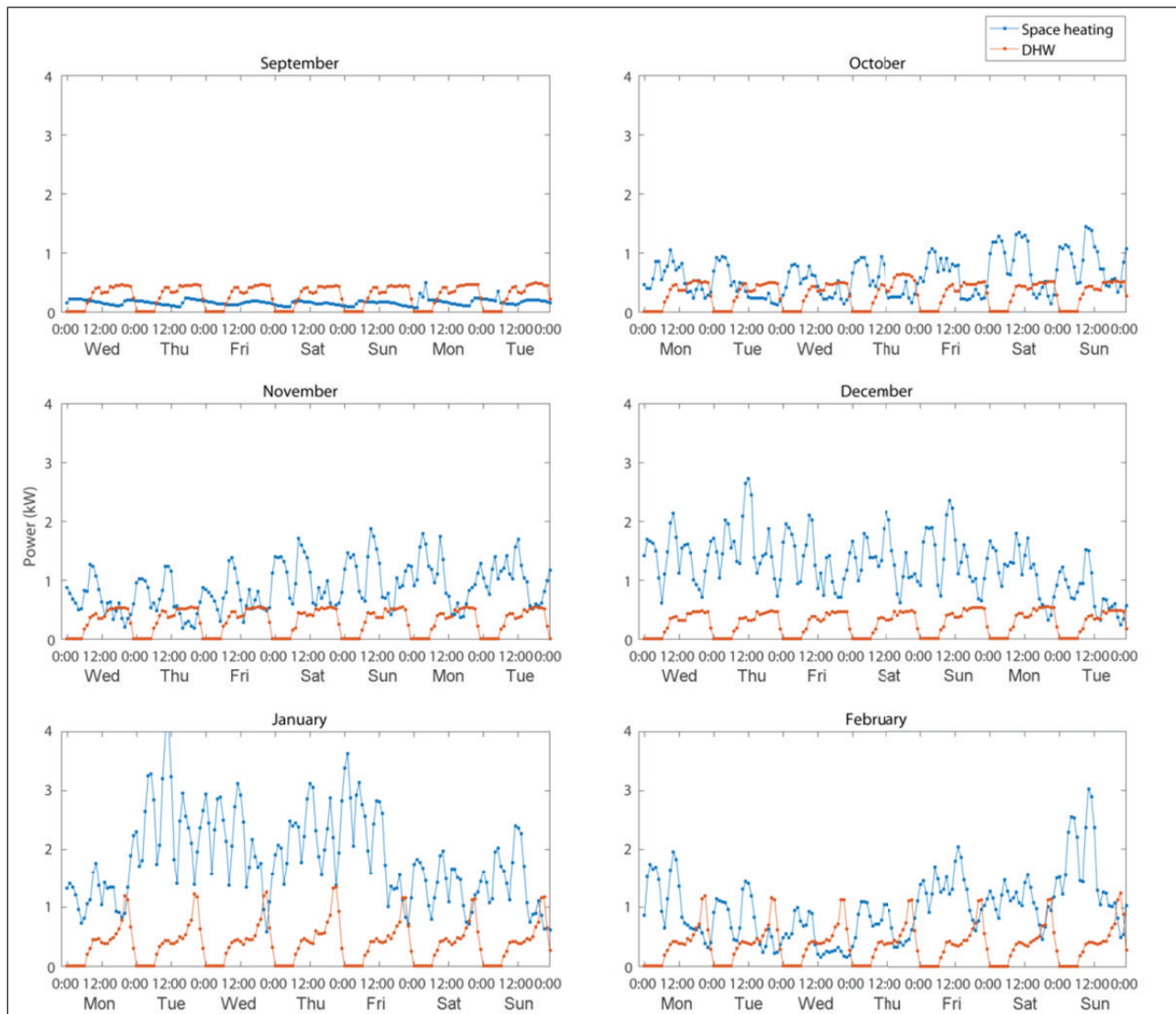


Figure 6: Hourly heat consumption data for the six studied periods.

peak loads reaching above 4 kW in January and averages ranging from around 500 W in October to 2 kW in January.

Energy Production

Electricity Production

The total amount of electricity produced locally by the platform was 250 kWh during the six studied periods in September–February, accounting for a little over 19% as a ratio to the total electricity consumption. The production for the studied periods is shown in **Figure 7**. The overall distribution between solar and wind energy was almost even, with 54% coming from the PV panels and 46% from the micro-wind turbine. Due to Finland being located far north, the distribution of the PV production among the different months was extremely bipolar with the two periods in September and October accounting for almost 85% of the total. For wind production, the trend was the opposite with the winter months being the most productive, but the disparity was not as large as for the solar part. It is worth noting that the battery pack had a

malfunction with its state-of-charge monitoring device, which may have resulted in loss of potential production due to the system thinking that the battery was fully charged whereas in reality there would have still been storage capacity left.

Electricity production data for the two periods in September and February is shown at one-minute resolution in **Figure 8** as examples of an autumn and winter period. The corresponding solar irradiance and wind speed data can be found in **Figures 9** and **10**, respectively. From these data, the intermittent and unpredictable nature of the renewable production is clearly observable. For PV, the shape and magnitude of the power peaks days were similar for each day during the September period whenever the sun was shining, with the peak power after the inverter being over 3 kW. Wind production, expectedly, did not follow any trends. The peak powers received from the micro-wind turbine on the most productive days were slightly smaller than from the PV and the production was heavily concentrated on a few windy days.

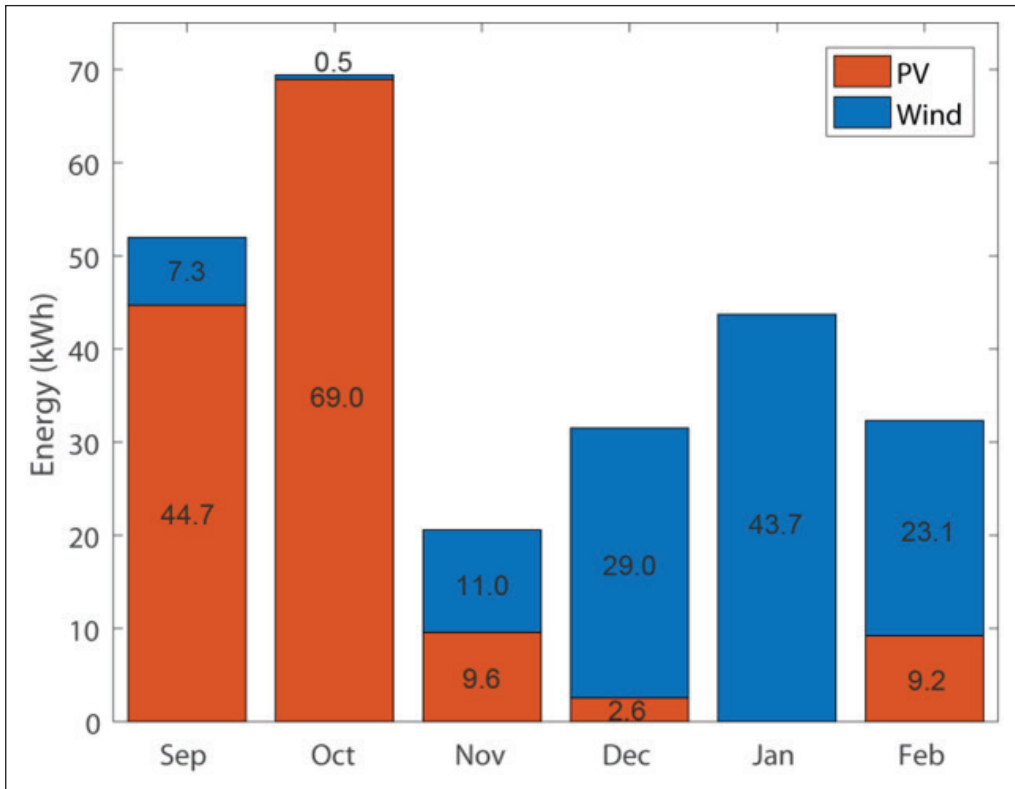


Figure 7: Electricity production for the six studied periods.

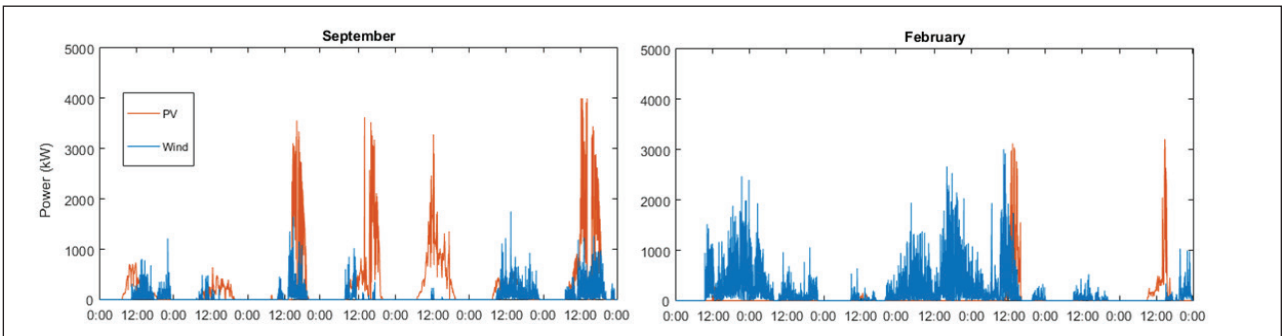


Figure 8: Electricity production during the two studied periods in September and February.

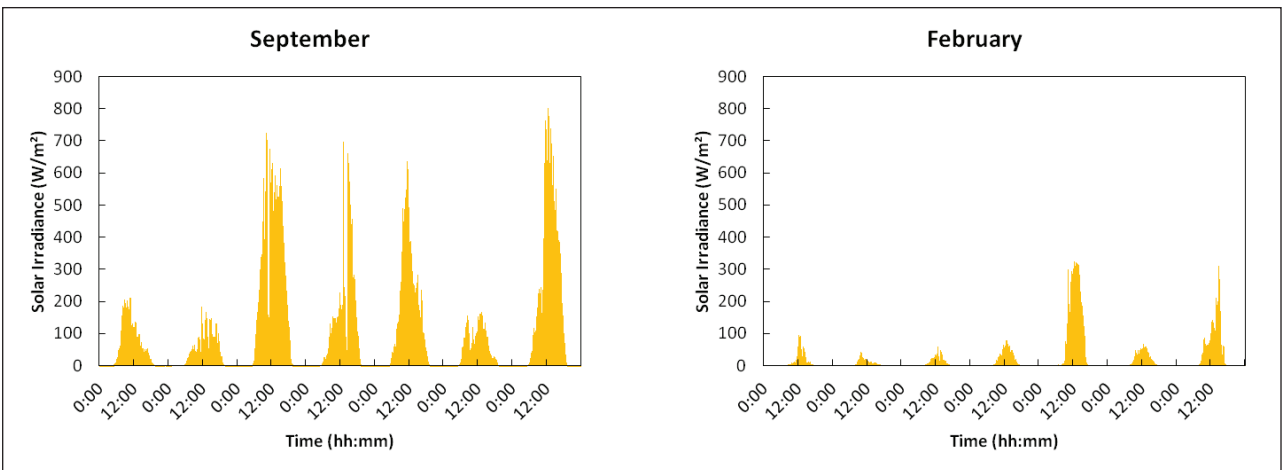


Figure 9: Solar irradiance during the two studied periods in September and February.

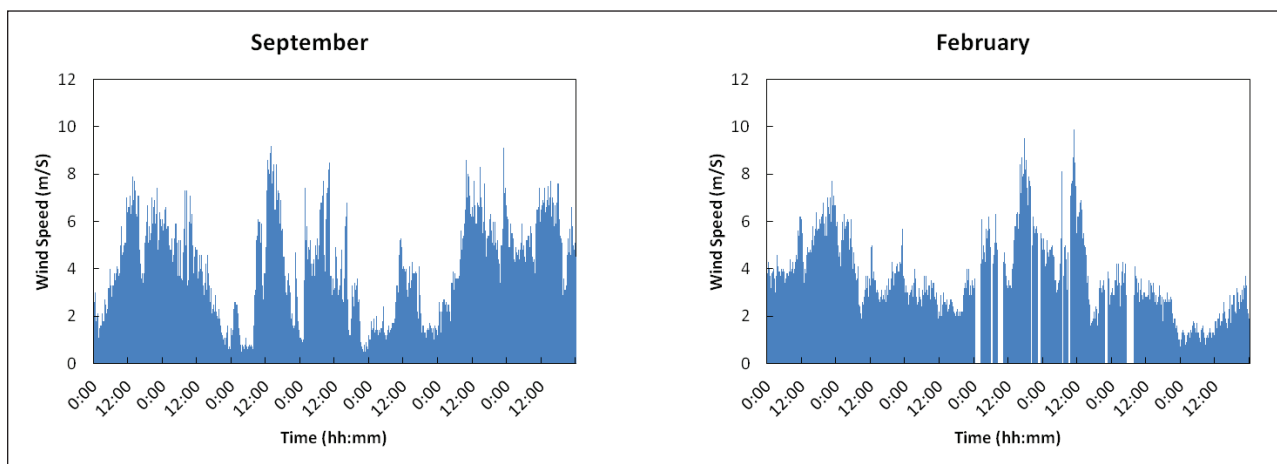


Figure 10: Wind speed during the two studied periods in September and February.

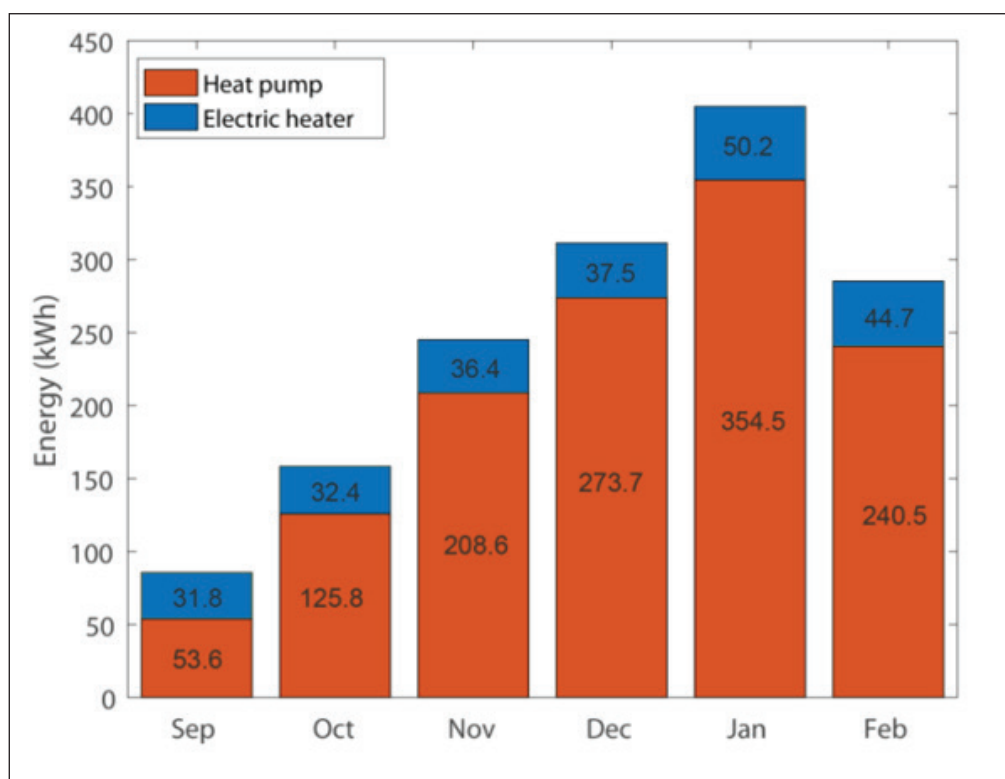


Figure 11: Heat production during the six studied periods.

Heat Production

Heat was produced entirely by the GSHP and the electric heater during the studied periods as there were some sensor problems with the solar thermal system. The GSHP accounted for most of the production as the electric heater was only used when the DHW temperature fell below 60°C. The total amount of heat produced during the six periods under investigation was 1490 kWh. Since the heating demand from the simulated building was 1280 kWh for the same period, it can be concluded that 14% of the generated heat was dissipated as heat loss from the storage tank and piping into the surrounding air.

The heat production is divided into monthly period values in Figure 11. It clearly follows the trends of the heating demand in Figure 5. The comparison of the amounts of the

generated heat to the electricity consumption in Figure 4 shows that the COP of the GSHP has some variation. During autumn the COP was roughly two whereas in the winter months it was slightly higher, about three. This can be explained by the compressor start-up period during which the unit consumes more electricity than during normal operation. Since the start-up period was the same in every operation cycle but the cycles in autumn were shorter than those in winter, this resulted in a larger fraction of operation under start-up conditions in autumn compared to winter.

Energy Matching

In the emulator, two different forms of energy (electricity and heat) are considered. However, since during this first phase of the emulator operation, the solar ther-

mal collectors were not in use and the ratios of locally generated/imported electricity were not recorded for the GHSP or the electric heater, the energy matching analysis was only done for the electric energy.

The simple comparison of total electricity generation (PV and wind) and total electrical demand (appliances, HP and electric heater) for each of the six periods depicted in **Figure 12** shows that the renewable generation covered roughly 35% of the total demand in September and October whereas the coverage during winter months was much less, around 10%. The hourly generation and consumption data presented in **Figure 13** reveal that especially during September and October when solar energy was available, the demand spikes rarely matched the production. In the winter months, production was much lower in general, and there was a steadier demand, resulting in a much better matching of the two.

To further evaluate the matching features of the energy generation and demand, the extended matching indices developed by Cao et al. are used (Cao, Hasan & Sirén 2013b). These indices are extended based on the

two basic matching indices- the on-site energy fraction (OEF) and the on-site energy matching (OEM). The OEF essentially indicates the proportion of the local demand which is covered by the on-site energy during a given time window whereas the OEM essentially indicates the proportion of the on-site generation which is consumed in the building and system rather than being exported or dumped. From a typical energy matching graph shown in **Figure 14**, the OEF can be obtained as the ratio of area III to the sum of areas I and III, and the OEM as the ratio of area III to the sum of areas II and III. The two basic indices of OEF and OEM were extended into six extended matching indices in the reference (Cao, Hasan & Sirén 2013b) by taking different energy forms, energy conversions, storages and hybrid grids connections into account: they are nomenclated as OEF_{e,h,c} and OEM_{e,h,c}, where the suffixes “e”, “h”, and “c” stand for the electrical, heating and cooling energy forms, respectively. Since only electrical energy is considered in this study, the extended matching indices for the electricity-“OEF_e” and “OEM_e”- are used here:

$$OEF_e = \frac{\int_{t_1}^{t_2} \text{Min}[G_{elec}(t) - ES_{on}(t) - I_e(t); L_{elec}(t) + E_{off-h}(t) + E_{on-h}(t) + E_{off-c}(t) + E_{on-c}(t)] dt}{\int_{t_1}^{t_2} [L_{elec}(t) + E_{off-h}(t) + E_{on-h}(t) + E_{off-c}(t) + E_{on-c}(t)] dt}$$

$$OEM_e = \frac{\int_{t_1}^{t_2} \text{Min}[G_{elec}(t); L_{elec}(t) + E_{on-h}(t) + E_{on-c}(t) + ES_{on}(t) + I_e(t)] dt}{\int_{t_1}^{t_2} G_{elec}(t) dt}$$

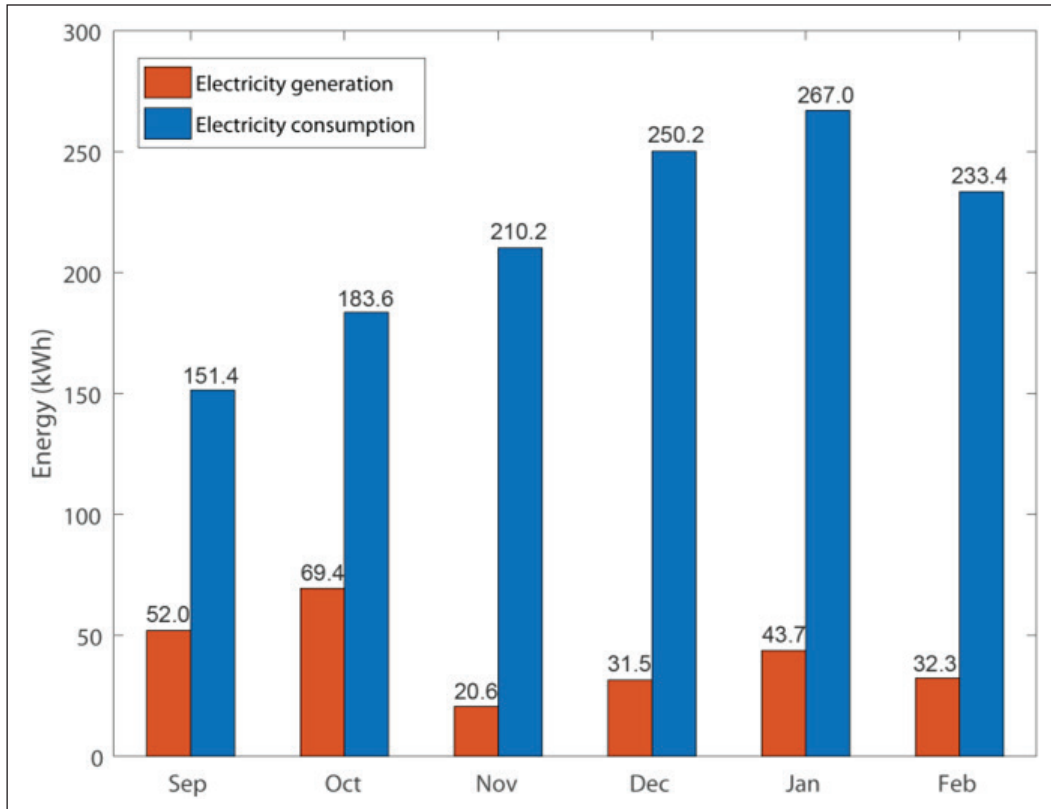


Figure 12: Comparison of total electricity generation and consumption during the six studied periods.

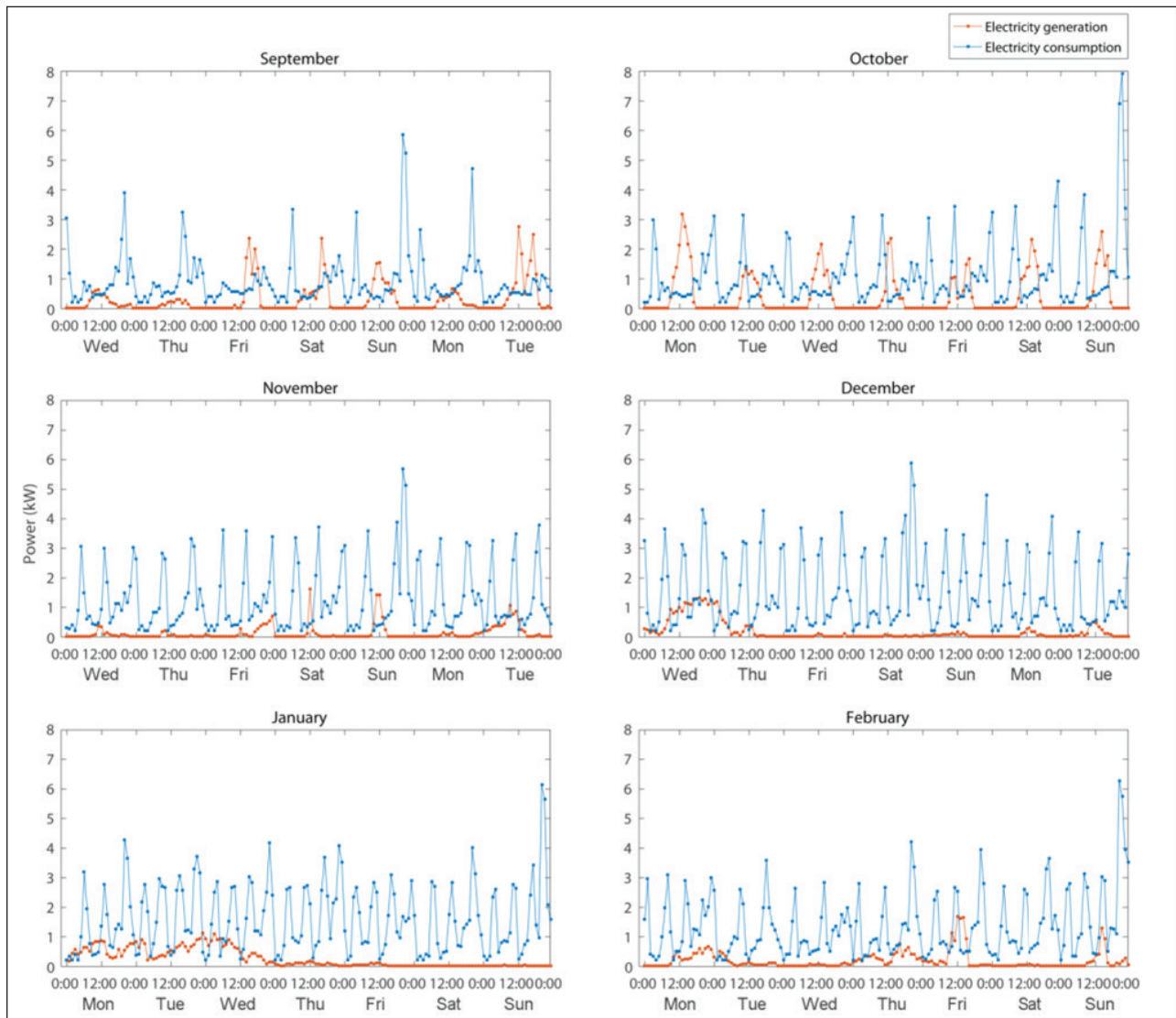


Figure 13: Hourly comparison of the total electricity production and consumption.

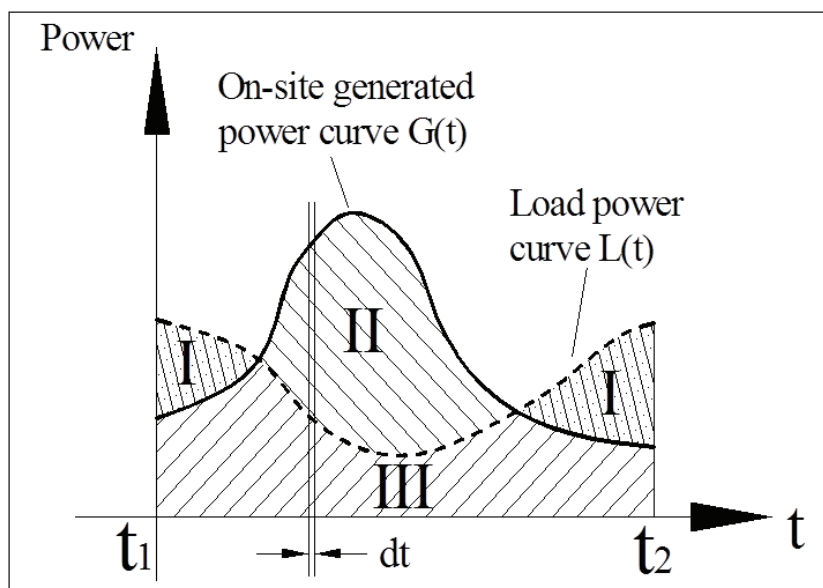


Figure 14: A brief illustration of the basic matching situation between load and generation with only one energy form (Cao, Hasan & Sirén 2013b).

where G_{elec} is the electrical power generated by the on-site electrical energy production system; ES_{on} is the net on-site part of the electrical power sent to electrical storage, where the charging and discharging processes are accounted in the “+” and “-” signs, respectively; I_e is the loss of on-site electrical power during the distribution process; L_{elec} is the electrical load power excluding the electrical load from the electrically driven heating and cooling machines; $E_{\text{off-h}}$ and $E_{\text{on-h}}$ are the off-site and on-site parts of the electrical power sent to the electrically driven heating machines, respectively; $E_{\text{off-c}}$ and $E_{\text{on-c}}$ are the off-site and on-site parts of the electrical power sent to the electrically driven cooling machines, respectively. Furthermore, in this specific study, the terms of $E_{\text{off-c}}(t)$ and $E_{\text{on-c}}(t)$ can be omitted, as there is no electrically driven chiller in the emulator system.

The hourly values of OEF_e and OEM_e for each period are presented in **Figure 15**. In September and October, OEF_e had a strong daily/nightly trend resulting from the local production being mostly from the PV system. In the wind-dominated winter months the behavior was much more irregular, with peaks often occurred around midnight

when the load was lower. Since electricity consumption was much larger compared to the local production, OEM_e was unity for most the time regardless of the time of the year. The only clear exceptions to this were the sunny September and October days around noon when the PV production could cover the entire load and even generate some excess. In winter time, there were a few very short periods – mostly during night time – when the wind generator produced more power than the building consumed.

As the matching indices are essentially integrals of time, the choice of the time step may have a major influence on the results. To investigate this, both OEF_e and OEM_e were calculated for each period with several different time steps ranging from five seconds to one week. The results, shown in **Figure 16**, reveal that in this case there was very little difference between time steps from five seconds up to one hour. However, going for a one-day or one-week time step resulted in completely different values, revealing that these two choices are clearly too coarse for this type of a study. Another interesting remark is that while the results within the time steps of one hour and below are mixed for OEF_e, choosing a longer time step seems

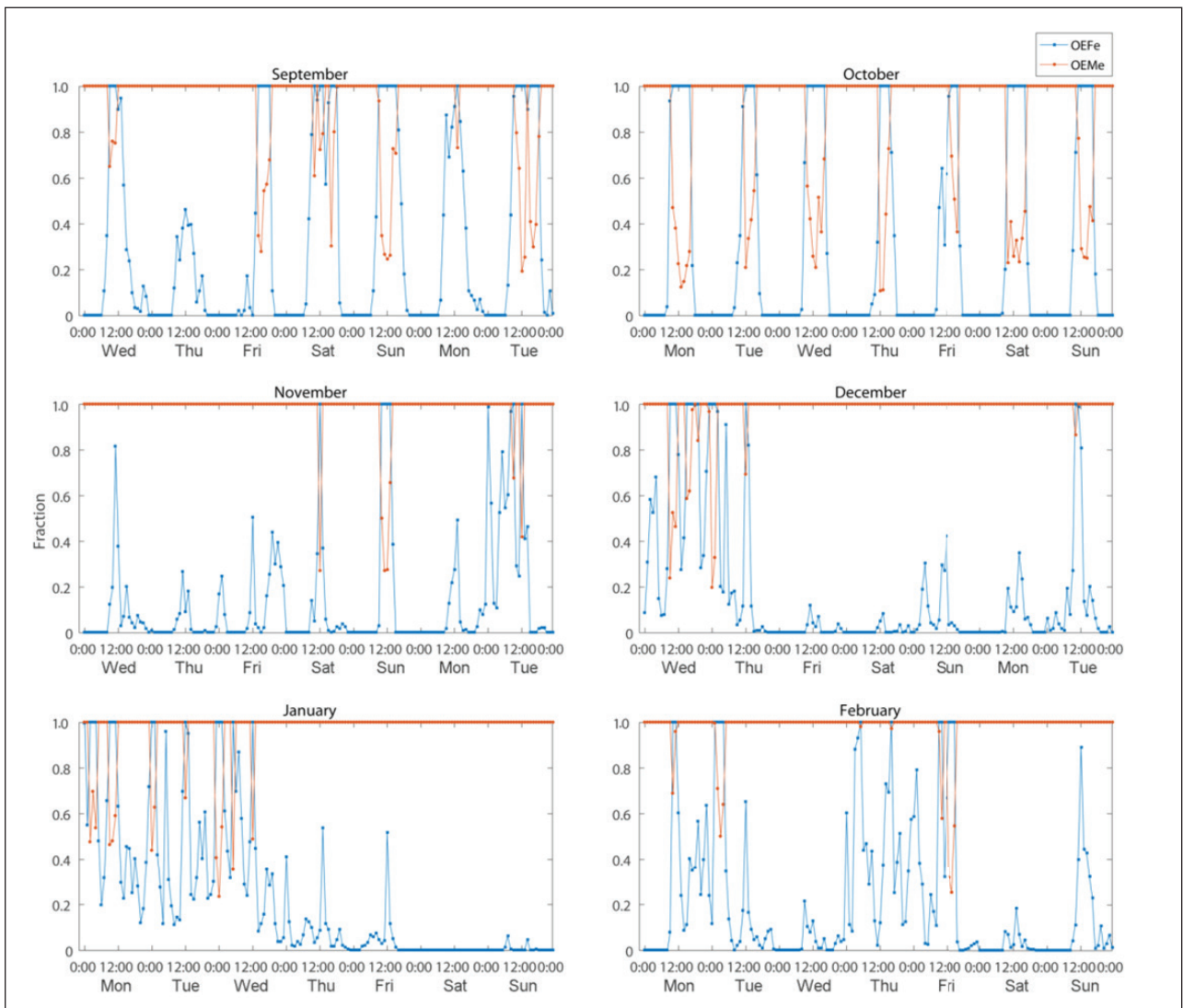


Figure 15: Hourly matching indices OEF_e and OEM_e.

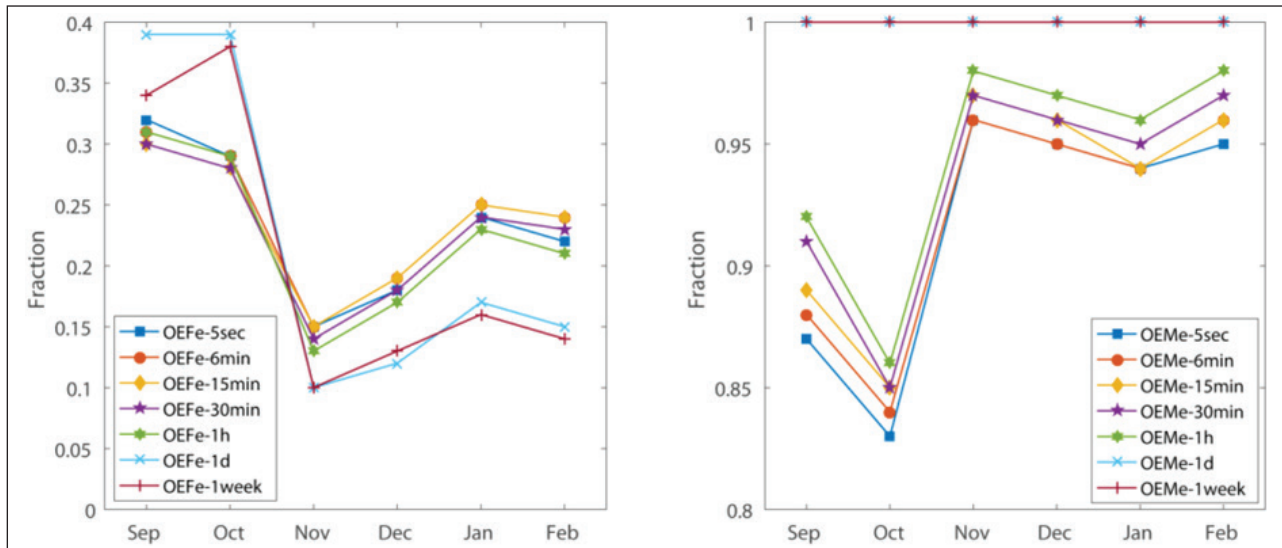


Figure 16: Matching indices OEFc and OMEc calculated with different time steps.

to consistently result in overestimation of OMEc. This is explained by short-time weather effects such as a small cloud blocking the sun or a sudden gust of wind being averaged out when the time step is larger.

Conclusions

In this study, the performance and energy matching features of a semi-virtual nearly-zero energy building emulator platform located at Aalto University in Espoo, Finland were evaluated during the first phase operation of the project. Six samples of seven-day periods, one per calendar month from September 2015 to February 2016, were chosen to represent the operation of the system in different climate conditions. The platform consists of a real part including renewable energy production (PV panels, micro-wind turbine and solar thermal collectors), storage (battery pack and hot water storage tank) and conversion (GSHP and electric heater) equipment, and a virtual part comprising the models of the building and the GSHP borehole. The system is operated by a Labview program, which is connected to more than 100 sensors and actuators in the real part, and to the TRNSYS simulation software, which is responsible for modeling the operation of the virtual part.

During the six studied periods, the total electricity demand was 1290 kWh, consisting of a 44/38/18% share between household appliances, GSHP and electric heater, respectively. The appliance load followed a similar trend every month, with peaks in the morning from six to nine and in the evening from 17 to 24, and a base load of 200 W. The electricity demand of the GSHP was expectedly much higher in the cold winter months, peaking at 119 kWh in January compared to 29 kWh in September. The electric heater was also utilized slightly more in the winter months. The electricity production was much less than the demand, only 250 kWh in total. A slight majority (54%) of that came from the PV plant whose production was dominated in September and October (85% share). The micro-wind turbine peaked in the winter months,

with December and January being the best ones for production. This kind of production bipolarity is typical for the Finnish climate with long daylight time in summer and most of the heavy winds occurring in autumn/winter. The heat demand for the studied periods was almost equal to the electricity demand, 1280 kWh. As there was no solar heat available, the demand was satisfied by the use of the GSHP and the electric heater whose combined production was 1490 kWh, indicating heat losses of around 14%.

The energy matching was evaluated for the electricity using the matching indices OEFc and OMEc. The OEFc showed a large day-night fluctuation in September and October due to the production coming from the PV plant. In wind-dominated winter time, there were no notable trends in OEFc. Due to poor production, the system could utilize most of the local production on-site, and thus OMEc was unity for most of the time. The PV peaks around noon in September and October, and some nightly short-term wind production in the winter months were the exceptions during which there was excess production to be stored in the battery.

As this was the first operation phase of the emulator, some oversights and problems were faced. For example, the building simulation was run on typical weather data and was not able to use the online data from a local weather station. Also, problems related to operating the solar thermal collector and the proper operation of the batteries were discovered. All these issues were solved in the second phase of operation of the emulator that started in fall 2016 and is still ongoing. In addition to the above, a connection was added to export surplus solar heat to an emulated district heating network. As well, an energy management system was developed and integrated in the emulator, where it uses an optimization algorithm to make online decisions at each time step on how to minimize the total energy cost (through energy conversion, storage or export) using information about the weather forecast for the next hours as well as electricity spot pricing.

Acknowledgements

This research is part of the project “Advanced Energy Matching for Zero-Energy Buildings in Future Smart Hybrid Networks”, which is mainly funded by the Academy of Finland.

Competing Interests

The authors have no competing interests to declare.

References

- Akvaterm Oy** 2014 *AKVA SOLAR brochure*. [Online] Available at: http://www.akvaterm.fi/files/akva_solar_0614_eng.pdf [Accessed 13 12 2017].
- Bussar, C**, et al. 2015 Large-scale Integration of Renewable Energies and Impact on Storage Demand in a European Renewable Power System of 2050. *Energy Procedia*, 73: 145–153. DOI: <https://doi.org/10.1016/j.egypro.2015.07.662>
- Cao, S, Hasan, A and Sirén, K** 2013a Analysis and solution for renewable energy load matching for a single-family house. *Energy and Buildings*, 65: 398–411. DOI: <https://doi.org/10.1016/j.enbuild.2013.06.013>
- Cao, S, Hasan, A and Sirén, K** 2013b On-site energy matching indices for buildings with energy conversion, storage and hybrid grid connections. *Energy and Buildings*, 64: 423–438. DOI: <https://doi.org/10.1016/j.enbuild.2013.05.030>
- Cao, S and Sirén, K** 2014 Impact of simulation time-resolution on the matching of PV production and household electric demand. *Applied Energy*, 128: 192–208. DOI: <https://doi.org/10.1016/j.apenergy.2014.04.075>
- Cao, S and Sirén, K** 2015 The influence of simulation time-resolution on the matching between on-site micro-wind generation and building electric demand. *Journal of Building Performance Simulation*, 9(5): 449–468. DOI: <https://doi.org/10.1080/19401493.2015.1077270>
- Delucchi, M A and Jacobson, M Z** 2011 Providing all global energy with wind, water and solar power, Part II: Reliability, system and transmission costs, and policies. *Energy Policy*, 39: 1170–1190. DOI: <https://doi.org/10.1016/j.enpol.2010.11.045>
- European Commission** 2017a *Buildings*. [Online] Available at: <https://ec.europa.eu/energy/en/topics/energy-efficiency/buildings> [Accessed 16 October 2017].
- European Commission** 2017b *Nearly zero-energy buildings*. [Online] Available at: <https://ec.europa.eu/energy/en/topics/energy-efficiency/buildings/nearly-zero-energy-buildings> [Accessed 16 October 2017].
- Finnish Ministry of the Environment** 2007 *Rakentamismääräyskokoelma D1*. Helsinki: Finnish Ministry of the Environment.
- Finnwind Oy** 2011 *Tuule E200 tuulivoimala – tekninen kuvaus*. [Online] [Accessed 25 11 2013, no longer available online].
- Finnwind Oy** 2017 *Finnwind*. [Online] Available at: www.finnwind.fi [Accessed 13 12 2017].
- Hirvonen, J, Kayo, G, Hasan, A and Sirén, K** 2016 Zero energy level and economic potential of small-scale building-integrated PV with different heating systems in Nordic conditions. *Applied Energy*, 167: 255–269. DOI: <https://doi.org/10.1016/j.apenergy.2015.12.037>
- IEA Annex 67** 2017 *Laboratory facilities used to test energy flexibility in buildings*. [Online] Available at: <http://annex67.org/media/1373/lab-description-report-first-edition.pdf> [Accessed 13 12 2017].
- Kalamees, T**, et al. 2012 Development of weighting factors for climate variables for selecting the energy reference year according to the EN ISO 15927-4 standard. *Energy and Buildings*, 47: 53–60. DOI: <https://doi.org/10.1016/j.enbuild.2011.11.031>
- Korkas, CD, Baldi, S, Michailidis, I and Kosmatopoulos, E B** 2016 Occupancy-based demand response and thermal comfort optimization in microgrids with renewable energy sources and energy storage. *Applied Energy*, 163: 93–104. DOI: <https://doi.org/10.1016/j.apenergy.2015.10.140>
- Krajačić, G, Duić, N and da Graça Carvalho, M** 2011 How to achieve a 100% RES electricity supply for Portugal? *Applied Energy*, 88(2): 508–517. DOI: <https://doi.org/10.1016/j.apenergy.2010.09.006>
- Lund, H, Marszal-Pomianowska, A and Heiselberg, P** 2011 Zero energy buildings and mismatch compensation factors. *Energy and Buildings*, 43(7): 1646–1654. DOI: <https://doi.org/10.1016/j.enbuild.2011.03.006>
- Luthra, S**, et al. 2014 Adoption of smart grid technologies: An analysis of interactions among barriers. *Renewable and Sustainable Energy Reviews*, 33: 554–565. DOI: <https://doi.org/10.1016/j.rser.2014.02.030>
- Oilon Group Oy** 2017 *Ground source heat pump – Oilon GT*. [Online] Available at: <https://oilon.com/oilon-home/products/ground-source-heat/EN/oilon-junior-gt/> [Accessed 13 12 2017].
- Pina, A, Silva, C and Ferrao, P** 2012 The impact of demand side management strategies in the penetration of renewable electricity. *Energy*, 41: 128–137. DOI: <https://doi.org/10.1016/j.energy.2011.06.013>
- Plessmann, G, Erdmann, M, Hlusiak, M and Breyer, C** 2014 Global Energy Storage Demand for a 100% Renewable Electricity Supply. *Energy Procedia*, 46: 22–31. DOI: <https://doi.org/10.1016/j.egypro.2014.01.154>
- RITAR Power** 2017 *RA Series Battery*. [Online] Available at: <http://www.ritarpower.com/battery/Reserve%20Power%20Battery/RA%20Series/> [Accessed 13 12 2017].
- Salom, J**, et al. 2014 Analysis of load match and grid interaction indicators in net zero energy buildings with simulated and monitored data. *Applied Energy*, 136: 119–131. DOI: <https://doi.org/10.1016/j.apenergy.2014.09.018>
- SMA Solar Technology AG** 2017 *Sunny Island 6.0H/8.0H*. [Online] Available at: <https://www.sma.de/en/products/battery-inverters/sunny-island-60h-80h.html> [Accessed 13 12 2017].

- Sorensen, B** 2007 A sustainable energy future: Construction of demand and renewable energy supply scenarios. *International Journal of Energy Research*, 32: 436–470. DOI: <https://doi.org/10.1002/er.1375>
- The University of Wisconsin** 2017 *TRNSYS 18 Features*. [Online] Available at: <http://sel.me.wisc.edu/trnsys/features/features.html> [Accessed 16 October 2017].
- Ueckerdt, F, Brecha, R and Luderer, G** 2015 Analyzing major challenges of wind and solar variability in power systems. *Renewable Energy*, 81: 1–10. DOI: <https://doi.org/10.1016/j.renene.2015.03.002>
- Wang, R, Wang, P, Xiao, G and Gong, S** 2014 Power demand and supply management in microgrids with uncertainties of renewable energies. *International Journal of Electrical Power & Energy Systems*, 63: 260–269. DOI: <https://doi.org/10.1016/j.ijepes.2014.05.067>
- Xue, X, Wang, S, Sun, Y and Xiao, F** 2014 An interactive building power demand management strategy for facilitating smart grid optimization. *Applied Energy*, 116: 297–310. DOI: <https://doi.org/10.1016/j.apenergy.2013.11.064>

How to cite this article: Kilpeläinen, S, Lu, M, Cao, S, Hasan, A and Chen, S. 2018 Composition and Operation of a Semi-Virtual Renewable Energy-based Building Emulator. *Future Cities and Environment*, 4(1): 1, pp. 1–14, DOI: <https://doi.org/10.5334/fce.7>

Submitted: 16 October 2017

Accepted: 20 December 2017

Published: 26 January 2018

Copyright: © 2018 The Author(s). This is an open-access article distributed under the terms of the Creative Commons Attribution 4.0 International License (CC-BY 4.0), which permits unrestricted use, distribution, and reproduction in any medium, provided the original author and source are credited. See <http://creativecommons.org/licenses/by/4.0/>.



Future Cities and Environment, is a peer-reviewed open access journal published by Ubiquity Press.

OPEN ACCESS